DOI: 10.61782/fa.2025.0140

FORUM ACUSTICUM
EURONOISE 2025

APPLICABILITY OF THE DISCONTINUOUS GALERKIN METHOD FOR OUTDOOR NOISE PROPAGATION SIMULATIONS

Florian Kraxberger[1*] **Johannes Heinz**[2] **Andreas Wurzinger**[1]
Manfred Kaltenbacher[1] **Stefan Schoder**[1] **Christian Adams**[1]
[1] Institute of Fundamentals and Theory in Electrical Engineering (IGTE), Graz University of Technology, Graz, Austria.
[2] Independent researcher, Munich, Germany.

ABSTRACT

Simulation of outdoor noise propagation is often performed using geometry-based methods. However, these methods typically lack the ability to accurately capture wave phenomena, such as diffraction, leading to limitations in the low-frequency range. This study investigates the application of the Discontinuous Galerkin (DG) method, a wave-based computational approach, for simulating acoustic wave propagation in the time domain within a large outdoor environment. The used implementation of the DG method supports high-order basis functions in space and uses a matrix-free approach for high computational efficiency suitable for computations on high-performance clusters. Preliminary results from DG simulations conducted in a geometrically complex outdoor setting are presented, demonstrating the potential of this method for accurate noise propagation analysis at low frequencies.

Keywords: Discontinuous Galerkin Method, Outdoor noise propagation, Acoustic simulation

1. INTRODUCTION

Outdoor noise propagation simulations often rely on geometry-based acoustic simulation methods, which are standardised in Europe in CNOSSOS-EU [1]. However, geometry-based simulation methods for outdoor sound propagation simulations have shortcomings in the low-frequency range [2, S. 118]. This is especially obvious when comparing geometry-based methods with wave-based methods, such as the Finite Element Method (FEM) [3]. Computational demands regarding memory (RAM) and processor (CPU) limit the applicability of FEM to outdoor noise propagation simulations. This contribution addresses some limitations of FEM and geometry-based methods by using the Discontinuous Galerkin (DG) method.

The DG method is the latest advance in acoustics simulations, particularly room acoustics [4–6]. Consequently, its applicability to outdoor noise problems seems promising. An implementation of the acoustic conservation equations in a high-order DG framework is provided in [7, 8]. Therein, the system of equations is implemented into the software framework *ExaDG* [9], which itself relies on the *deal.II*-framwork [10]. The implementation uses a matrix-free approach [11], meaning that little to no RAM is required for the computations because the operator equations are computed on the fly. In contrast, with a conventional matrix-based approach, the matrices must be assembled before solving the system of equations as a whole.

This contribution investigates the applicability of the DG method to a 3D outdoor noise propagation scenario. A realistic outdoor noise propagation scenario is achieved by extruding the 2D geometry of our former study [3] for $D = 300\,\mathrm{m}$ to form a simple three-dimensional geometry, as shown in Fig. 1. The applicability of the DG method in the current implementation status is documented as a feasibility study.

This paper is organised as follows. In Sec. 2, the DG method is introduced and its application to a large-scale outdoor noise problem is discussed. In Sec. 3, preliminary results are presented, highlighting the applicability of

*Corresponding author: kraxberger@tugraz.at.
Copyright: ©2025 Kraxberger et al. This is an open-access article distributed under the terms of the Creative Commons Attribution 3.0 Unported License, which permits unrestricted use, distribution, and reproduction in any medium, provided the original author and source are credited.

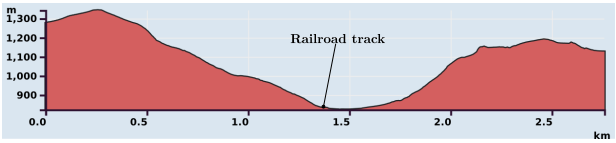

Figure 1. Two-dimensional cross-section through an alpine valley presented in [3, Fig. 2]. The railroad is considered the noise source. The 2D cross-section is extruded with an extrusion depth of $D = 300\,\mathrm{m}$ to form a 3D geometry.

the DG method. Section 4 provides a conclusion and an outlook to potential future developments.

2. DISCONTINUOUS GALERKIN METHOD FOR OUTDOOR NOISE PROPAGATION

The acoustic conservation equations are a set of two coupled first-order partial differential equations with the acoustic pressure p_a and acoustic particle velocity $\vec{u}_\mathrm{a}$ as solution quantities. In their strong form, conservation of mass and conservation of momentum are respectively defined as [7, Eq. (2.10)]

$$\frac{1}{c^2}\frac{\partial p_\mathrm{a}}{\partial t} + \rho_0 \nabla \cdot \vec{u}_\mathrm{a} = f \tag{1}$$

and

$$\rho_0 \frac{\partial \vec{u}_\mathrm{a}}{\partial t} + \nabla p_\mathrm{a} = \vec{0}\,, \tag{2}$$

where c is the speed of sound in air, ρ_0 is the ambient density of air, and f is an arbitrary source term. The air is assumed to be homogeneous and at rest.

2.1 Discontinuous Galerkin Formulation

To obtain the DG formulation of the acoustic conservation equations, Eq. (1) is multiplied with a scalar test function q_h, and Eq. (2) is multiplied with a vectorial test function $\vec{w}_h$. Furthermore, the equations are integrated over the volume of one element Ω_e, and integration by parts is applied on both equations. Furthermore, a second integration by parts is performed on the conservation of momentum equations such that a skew-symmetric formulation is achieved [12]. Introducing the jump terms $p^*_{\mathrm{a},h}$ for acoustic pressure and $\vec{u}^*_{\mathrm{a},h}$ for acoustic particle velocity, the weak DG formulation yields

$$\begin{aligned}\left(q_h, \frac{\partial p_{\mathrm{a},h}}{\partial t}\right)_{\Omega_e} - \left(\nabla q_h, \rho_0 c^2 \vec{u}_{\mathrm{a},h}\right)_{\Omega_e} \\ + \left(q_h \vec{n}, \rho_0 c^2 \vec{u}^*_{\mathrm{a},h}\right)_{\partial\Omega_e} = \left(q_h, c^2 f\right)_{\Omega_e}\end{aligned} \tag{3}$$

$$\begin{aligned}\left(\vec{w}_h, \frac{\partial \vec{u}_{\mathrm{a},h}}{\partial t}\right)_{\Omega_e} + \left(\vec{w}_h, \frac{1}{\rho_0}\nabla p_{\mathrm{a},h}\right)_{\Omega_e} \\ + \left(\vec{w}_h \cdot \vec{n}, \frac{1}{\rho_0}\left(p^*_{\mathrm{a},h} - p_{\mathrm{a},h}\right)\right)_{\partial\Omega_e} = \vec{0}\,.\end{aligned} \tag{4}$$

Therein, the compact notation for volume and surface integrals is used, such that $(a,b)_{\Omega_e} = \int_{\Omega_e} a \cdot b \,\mathrm{d}\Omega$ and $(a,b)_{\partial\Omega_e} = \int_{\partial\Omega_e} a \cdot b \,\mathrm{d}\partial\Omega$, where $\partial\Omega$ denotes the boundary of the volume Ω. Furthermore, the jump operators for an arbitrary quantity a are denoted as

$$\begin{aligned}\{\!\{a^*\}\!\} &= \frac{1}{2}\left(a^- + a^+\right)\,, \\ [\![a^*]\!] &= a^- \times \vec{n}^- + a^+ \times \vec{n}^+\,,\end{aligned} \tag{5}$$

where the superscript $^+$ denotes the solution in the adjacent element, and $^-$ denotes the solution in the current element. Therewith, the jump terms $p^*_{\mathrm{a},h}$ and $\vec{u}^*_{\mathrm{a},h}$ can be defined. Lax-Friedrichs fluxes are often used as jump terms, e.g., [5, 7], providing the advantage that they only depend on known material parameters of air, such that

$$\begin{aligned}p^*_{\mathrm{a},h} &= \{\!\{p_{\mathrm{a},h}\}\!\} - \tau [\![p_{\mathrm{a},h}]\!]\,, \\ \vec{u}^*_{\mathrm{a},h} &= \{\!\{\vec{u}_{\mathrm{a},h}\}\!\} - \gamma [\![\vec{u}_{\mathrm{a},h}]\!]\,,\end{aligned} \tag{6}$$

where $\tau = \rho_0 c/2$ and $\gamma = 1/(2\rho_0 c)$.

2.1.1 Boundary Conditions

A sound-hard boundary condition is applied to the ground (bottom surface) to have a simple test case, and first-order absorbing boundary conditions are applied to all other surfaces. This is achieved using the admittance boundary condition from [7, Sec. 3.2].

2.1.2 Time Stepping

The purely explicit time-stepping algorithm used in this work consists of an *Adams-Bashforth* predictor and an *Adams-Moulton* corrector, as defined in [7, Sec. 3.4.1]. The time step size Δt is based on the *Courant-Friedrichs-Lewy* (CFL) condition, such that

$$\Delta t = \frac{\mathrm{Cr}_f}{p^{1.5}} \frac{h_f}{c}\,, \tag{7}$$

where the CFL number is chosen to be $\mathrm{Cr}_f = 0.25$, p is the polynomial order, and h_f is the size of the smallest cell. This results in a time step size of $\Delta t \approx 2.5\,\mu\mathrm{s}$.

2.2 Spatial Discretisation

The discretization is based on the maximum element size $h_{\max}$ after an optional refinement. Following the inequality of Ainsworth [13] with the modification by Heinz [7, Eq. (3.22)], an upper frequency limit $f_{\max}$ is established based on the spatial order p. In Fig. 2, the upper frequency limit depending on the element size $h_{\max}$ is depicted for different spatial orders p. Based on these considerations, a

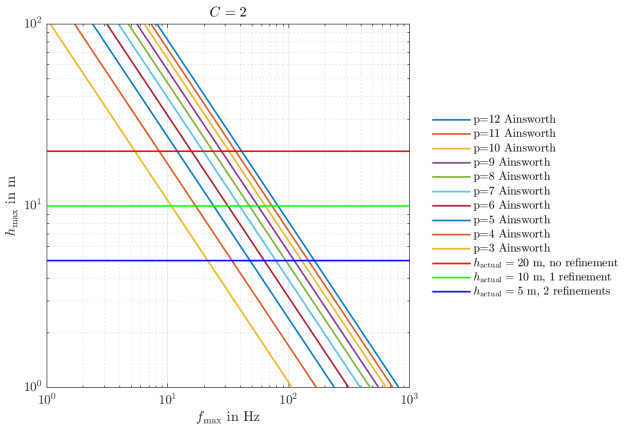

Figure 2. Maximum frequency $f_{\max}$ for which the spatial discretization fulfils the Ainsworth inequality with $C = 2$ following [7, Sec. 3.8.1].

spatial discretization with the element size $h_{\max} = 20\,\mathrm{m}$ is chosen together with one refinement and the spatial order $p = 8$. This yields an effective element size of $10\,\mathrm{m}$ and thus an upper frequency limit of approximately $f_{\max} = 80\,\mathrm{Hz}$. Furthermore, threefold refinement is applied in the region around the source to resolve the omnidirectional source term properly. The mesh has 297 752 eighth-order hexahedral elements. Each element has 2 916 degrees of freedom per cell, hence the system of equations has 868 244 832 degrees of freedom. Figure 3 shows the mesh used for the computations. The outer dimensions of the geometry are approximately $2700\,\mathrm{m}$ in length (x-direction), $600\,\mathrm{m}$ in height (y-direction), and $300\,\mathrm{m}$ in depth (z-direction).

3. PRELIMINARY RESULTS

The excitation signal can be chosen arbitrarily. For first evaluations, a spatially static sinusoidal excitation signal with a frequency of $f_{\mathrm{exc}} = 40\,\mathrm{Hz}$ is used. The results have been computed on the *Vienna Scientific Cluster* (VSC)

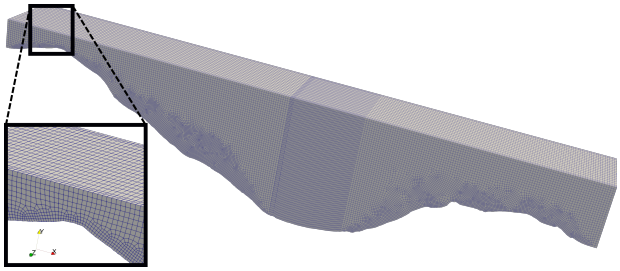

Figure 3. Spatial discretization of the computational domain.

[1] using 512 CPU threads with a wall time of 18 h (approximately 348 000 time steps following Eq. (7)). Figure 4 illustrates the field plot of the sound pressure level $L_p = 10\log_{10}\left(p^2/p_0^2\right)\,\mathrm{dB}$, $p_0 = 20\,\mu\mathrm{Pa}$, at $t = 0.87\,\mathrm{s}$.

4. DISCUSSION AND CONCLUSION

The results show that using the DG method for outdoor noise computations in large three-dimensional geometries allows for the computation of physically accurate results. This is enabled by the matrix-free implementation of the DG approach [11], allowing for parallelised computations on high-performance computing clusters. While the DG method is computationally more demanding than geometry-based methods, it still serves as a valuable tool for achieving precise wave-based predictions in the low-frequency range.

The algorithm is planned to be developed further to improve its applicability to outdoor noise problems. Regarding the source term, parametrised synthetic moving traffic noise can be incorporated such that the excitation signal is, e.g., road, railway, or aircraft noise with arbitrary trajectories. Furthermore, the efficiency of the algorithm can be improved by implementing a local time stepping (LTS) scheme, such as in [14], in the source region. The smallest element sizes occur in the source region, raising the need for a very small *global* time step according to Eq. (7) in the current implementation. A LTS algorithm would help to reduce the computational cost because the small time step is only necessary in regions with small elements. Finally, reflections of the tangential component of the acoustic pressure at the absorbing boundary condition are currently present. These may be tackled by employing a perfectly matched layer as a non-reflecting boundary condition.

[1] VSC5 with AMD EPYC 7713 (Milan) CPUs, *deal.II* version 9.7.0, *gcc* version 8.5.0 and the latest *ExaDG* version.

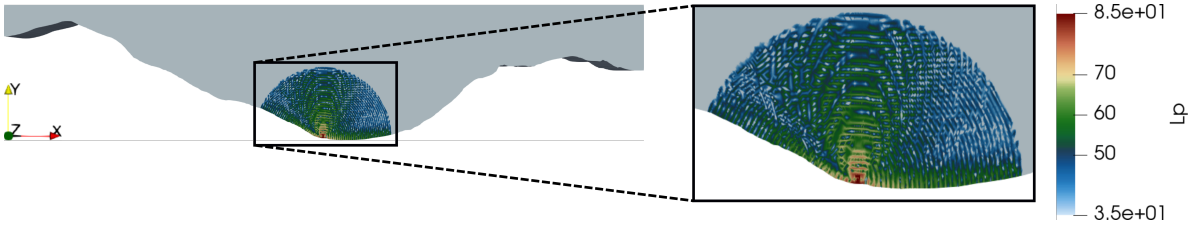

Figure 4. Field plot of the sound pressure level L_p at $t = 0.87\,\mathrm{s}$.

5. ACKNOWLEDGMENTS

F. K., M. K., and C. A. acknowledge support from the *"BMK Endowed Professorship on Noise Impact Research: Competence Center for Traffic Noise and Health"* of the Austrian Research Promotion Agency (FFG) under project No. FO999891611. The computational results presented have been achieved using the Vienna Scientific Cluster (VSC).

6. REFERENCES

[1] S. Kephalopoulos, M. Paviotti, and F. Anfosso-Lédée, "Common noise assessment methods in Europe (CNOSSOS-EU)," 2012.

[2] K. Attenborough, "Sound Propagation in the Atmosphere," in *Springer Handbook of Acoustics* (T. D. Rossing, ed.), Springer Handbooks, pp. 117–155, New York, NY: Springer New York, 2014.

[3] F. Kraxberger, C. Adams, J. Donnerer, M. Kaltenbacher, and S. Schoder, "Comparing outdoor sound propagation simulations based on geometrical and numerical methods," in *Proc. of Inter-Noise 2024*, (Nantes, France), pp. 2719–2730, International Institute for Noise Control Engineering, Aug. 2024.

[4] A. G. Prinn, "A Review of Finite Element Methods for Room Acoustics," *Acoustics*, vol. 5, pp. 367–395, Apr. 2023.

[5] H. Wang, I. Sihar, R. Pagán Muñoz, and M. Hornikx, "Room acoustics modelling in the time-domain with the nodal discontinuous Galerkin method," *J. Acoust. Soc. Am.*, vol. 145, pp. 2650–2663, Apr. 2019.

[6] W. Wittebol, H. Wang, M. Hornikx, and P. Calamia, "A hybrid room acoustic modeling approach combining image source, acoustic diffusion equation, and time-domain discontinuous Galerkin methods," *Appl. Acoust.*, vol. 223, p. 110068, July 2024.

[7] J. Heinz, *High-Order Discontinuous Galerkin Methods for Computational Acoustics and Aeroacoustics*. PhD thesis, TU Wien, 2023.

[8] J. Heinz, P. Munch, and M. Kaltenbacher, "High-order non-conforming discontinuous Galerkin methods for the acoustic conservation equations," *Int. J. Numer. Methods Eng.*, vol. 124, pp. 2034–2049, May 2023.

[9] D. Arndt, N. Fehn, G. Kanschat, K. Kormann, M. Kronbichler, P. Munch, W. A. Wall, and J. Witte, "ExaDG: High-Order Discontinuous Galerkin for the Exa-Scale," in *Software for Exascale Computing - SPPEXA 2016-2019* (H.-J. Bungartz, S. Reiz, B. Uekermann, P. Neumann, and W. E. Nagel, eds.), vol. 136, pp. 189–224, Cham: Springer International Publishing, 2020.

[10] D. Arndt, W. Bangerth, M. Bergbauer, M. Feder, M. Fehling, J. Heinz, T. Heister, L. Heltai, M. Kronbichler, M. Maier, P. Munch, J.-P. Pelteret, B. Turcksin, D. Wells, and S. Zampini, "The deal.II Library, Version 9.5," *J. Numer. Math.*, vol. 31, pp. 231–246, Sept. 2023.

[11] M. Kronbichler and K. Kormann, "Fast Matrix-Free Evaluation of Discontinuous Galerkin Finite Element Operators," *ACM Trans. Math. Softw.*, vol. 45, pp. 1–40, Sept. 2019.

[12] J. Heinz, P. Rucz, M. Ulveczki, A. Wurzinger, M. Kaltenbacher, and S. Schoder, "Verifying computational aeroacoustic solvers by the co-rotating vortex pair," 2025. Manuscript in preparation.

[13] M. Ainsworth, "Discrete Dispersion Relation for *hp* -Version Finite Element Approximation at High Wave Number," *SIAM J. Numer. Anal.*, vol. 42, pp. 553–575, Jan. 2004.

[14] H. Wang, M. Cosnefroy, and M. Hornikx, "An arbitrary high-order discontinuous Galerkin method with local time-stepping for linear acoustic wave propagation," *J. Acoust. Soc. Am.*, vol. 149, pp. 569–580, Jan. 2021.